

9-21-2021

Investigations of Cracking Mechanisms of Sport City Overpass Bridge by the FE Method.

A. Al-Rodan

Department of Civil Engineering, Mutah University., JORDAN.

Follow this and additional works at: <https://mej.researchcommons.org/home>

Recommended Citation

Al-Rodan, A. (2021) "Investigations of Cracking Mechanisms of Sport City Overpass Bridge by the FE Method.," *Mansoura Engineering Journal*: Vol. 28 : Iss. 3 , Article 13.

Available at: <https://doi.org/10.21608/bfemu.2021.141773>

This Original Study is brought to you for free and open access by Mansoura Engineering Journal. It has been accepted for inclusion in Mansoura Engineering Journal by an authorized editor of Mansoura Engineering Journal. For more information, please contact mej@mans.edu.eg.

INVESTIGATIONS OF CRACKING MECHANISMS OF SPORT CITY OVERPASS BRIDGE BY THE FE METHOD

دراسة التشققات في جسر تقاطع المدينة الرياضية باستخدام طريقة
العناصر المحددة

A. Al-Rodan

Assistant professor, Department of Civil Engineering,
Mutah University. JORDAN, Email: akrodan@mutah.edu.jo

خلاصة

في هذه البحث تم استخدام طريقة العناصر المحددة في دراسة الجسور الفرسجية المصنعة بطريقة الإجهاد المسبق. بعض التشققات الناتجة عن أجهاد القص تم ملاحظتها في جسر تقاطع المدينة الرياضية الذي تم بنائه قرب مدينة الحسين للشباب في نهاية السبعينات وما زال يستخدم إلى يومنا هذا. طريقة المحاكاة العددية استخدمت لدراسة هذه التشققات ومعرفة أسبابها. النتائج التي تم الحصول عليها تم تحليلها ومقارنتها مع ما تم ملاحظته في الموقع، وتؤكد أنه يمكن استخدام طريقة العناصر المحددة غير الخطية لدراسة الجسور المصنعة بطريقة الإجهاد المسبق.

ABSTRACT

This paper describes the finite-element modeling philosophy employed for the analysis of a long span bridge constructed using prestressed composite girder technology. The structure has been in service since late 1970's, and has innumerable visible shear cracks originating near the supports. The present investigation has been under taken in order to identify the possible mechanisms for the shear cracks. The ABAQUS finite-element package is used to simulate and identify the possible mechanism for the shear cracks under dead and live load (traffic load). The results obtained from the finite-element analysis are evaluated and the effectiveness of the model is assessed by comparison of the crack patterns of the numerical results and the observations. Some conclusions are made on the cracking mechanisms.

KEYWORDS: cracking mechanisms, bridge, prestressed, finite element.

INTRODUCTION

There are more than 100 bridges in Jordan and approximately 30% of them need to be repaired. Cracks are the basic signs showing distress in most long span bridges constructed using prestressing technology, and understanding the cracking mechanisms help engineers to diagnose bridge problems. In many cases, those structures are constructed by post tensioning together pre-cast girder cross-sections. For example, there is longitudinal post tensioning in the top and bottom slab over the support and mid-span respectively, also a transverse post

tensioning in the top of the deck. Shear strength, as designed, is provided by the concrete and shear reinforcement. Such composite sections have been shown to provide excellent stability during construction and in service period due to their high torsional rigidity (6). Design of joints between segments is the key technology to ensure high torsional rigidity. A typical design is to use shear keys which provide shear strength and guarantee the segments to be locked into place. However, due to the geometrical profile of the bridge, there will be stress concentration near the support under dead and live loads. This gives a major reason of crack propagation near the support of the bridge.

The Sport City Bridge, shown in Fig. 1, is one of the examples with severe cracks near the support. This is a 313m, continuous post tensioned bridge built in the late 1970's. The structure started showing signs of distress very early in its service life and numerous shear cracks have been developed in the web (2). Fig. 2 shows a cracking pattern which gives out a general idea of the crack propagation which has occurred in the middle span of the bridge. The figure shows that extensive cracking was observed near pier 5, and the severity of the cracks reduces towards the center of the span. The maximum crack may open as large as 0.1 to 0.3mm according to our measurement. Almost no crack can be found near the middle of the span. The most severe cracks are located near the piers. The observed crack patterns are relatively unusual for such post-tensioned bridge, which is supposed to have a very high torsional rigidity (7). In this paper, a three dimensional finite element model using the finite element program ABAQUS is presented. The cracking mechanism is analyzed based on the model.

FINITE ELEMENT METHOD

The finite element is a useful tool for the analysis of problems with complex geometry, material properties, and boundary conditions. The technique can produce comprehensive and reliable results if the method is used correctly. It is much cheaper than a full-scale experimental testing. An accurate model to simulate the actual structure is necessary in order to accomplish a successful analysis.

The commercial multipurpose finite-element software package ABAQUS (1) is employed in this research. In the finite-element models described herein, both geometrical and material

nonlinearities are considered. These nonlinearities tend to create formidable computing requirements since dense meshes of brick elements must be used to properly model localized instabilities that occur in conjunction with global instabilities, both of which are inelastic in nature.

ABAQUS is widely recognized as being a very appropriate tool for use in structural analysis problems involving a high degree of geometric and material nonlinearity. The pre- and postprocessing work was achieved by ABAQUS/CAE version 6.2, which is an additional module written to enhance ABAQUS. It is a graphical user interface program that allows user to execute a finite-element analysis process from start to finish. The FE model can be viewed and checked interactively and the results (stress, displacements, etc.) can be visualized graphically.

FINITE ELEMENT MODEL

Several finite element models (5 spans, 2 and half spans and half spans) have been simulated in order to reach different goals (eigenvalue analysis, crack propagating simulation). In this paper, to understand the cracking mechanism of the bridge, one interior span between piers 4 and 5 has been modeled, (Fig. 1). The model has attempted to simulate the bridge as realistic as possible. The cross sectional dimensions of the bridge middle span shown in Fig. 3, which taken from the design drawings, were used to build up the FE model. Post tensioning tendons and their corresponding prestressing forces are introduced by incorporating reinforcing element (rebar elements, ABAQUS library). By making use of symmetry in loading and geometry, only quarter of the interior span need to be modeled in order to reduce the computational time (Fig. 4). The boundary conditions on the planes of symmetry have been applied as follows: the nodal displacement perpendicular to the plane of symmetry is restrained while the two remaining translational degrees of freedom are free; the nodal rotation perpendicular to the plane of symmetry is free while the two remaining rotational degrees of freedom are restrained. To model the bridge, eight-nodes linear 3D brick element were utilized. These elements are of type C3D8 in ABAQUS terminology. Rebar elements were used to model the steel. The model has been discretized into 6120 brick element and more than 10000 rebar elements. The material

properties used for the model were determined from the engineering stress strain-curve. The incorporation of material nonlinearity in an ABAQUS model requires the use of the true stress (σ_{true}) versus the logarithmic plastic strain (ϵ_{in}^{pl}) relationship. This must be determined from the engineering stress-strain relationship using:

$$\sigma_{true} = \sigma_{eng} (1 + \epsilon_{eng}) \dots\dots\dots 1$$

$$\epsilon_{in}^{pl} = \ln(1 + \epsilon_{eng}) - \frac{\sigma_{true}}{E} \dots\dots\dots 2$$

in which σ_{eng} is the engineering stress; and ϵ_{eng} is the engineering strain (HKS 2002).

Table 1; Material Properties for the Bridge

Concrete		Prestressing Tendon	
Young's modulus:	32.7 kN/mm ²	Young's modulus:	195 kN/mm ²
Poisson ratio:	0.2	Density:	7.5x10 ³ kg/m ³
Density:	2.45x10 ³ kg/m ³	Prestress:	2226kN for 12 strands
Yield stress:	35.5N/mm ²	Strand diameter:	15.7mm
Failure stress:	47.5N/mm ²		
Strain failure:	3x10 ³		

INVESTIGATION OF CRACK PROPAGATION

Initial Contact Model

In order to detect crack initiation and propagation, a simple cracking criterion is used. This criterion states that a crack forms when the maximum principle tensile stress exceeds the tensile strength of the brittle material. In the finite element model, both Mode I and Mode II fracture are taken into consideration by using brittle cracking model provided in ABAQUS-Explicit. For the case considered in current analysis, the post failure stress strain relationship shown in Fig. 6 was adopted. Although the strain at failure in standard concrete is typically 10⁻⁴, the

value used as tension failure strain of the concrete in our computation is 10^{-3} . This value based on the fact of the reinforcement of the bridge.

As a first step of the finite element simulation, a nonlinear continuum analysis was carried out for the model to estimate the magnitude of superimposed live load required for any element of the structure to reach a failure stress of 47.5 MPa. A uniformly distributed load was placed on top of the deck, which has a surface area of approximately 89.4m^2 . It was found that for such a failure to occur a superimposed live load of 162 tonnes, is needed to be applied over this surface area, with an average pressure of 18.98kN/m^2 , which is a very high value for any traffic conditions. Moreover, the direction of the principal stresses obtained in the web does indicate if the concrete is weak enough, which shows that it maybe possible for a crack to propagate in a pattern similar to those observed at site. Figs. 10 & 11 show the shear stress distribution on the bridge deck. The stress concentration is similar to the cracks initiation and propagation in the bridge. The cracks initiate at the web keep going up passing mid-depth of the bridge. Although the location of the cracks is similar to what was observed on the bridge, the simulated results are different from the actual situation, and, as mentioned above, the supposed superimposed live loads 162 tonnes would never happen on the bridge. This means that in order to correlate the observed cracks of the bridge, there is still something hidden behind, and the above intact model needs to be modified. By noticing the crack plot shown in Fig. 2, it is a reasonable assumption that initial weakness or even tiny cracks may have happened near the shear keys close to the support. This gives us the following modified weakened model.

Modified Weakened Model

The aim of this model is to develop a FE model for the bridge, which exhibits a behavior (cracks pattern) similar to that in practice under super imposed live load (traffic loading). In this model it was assumed that several elements near the shear keys close to support (pier 5) have been weakened and the tensile strain in the concrete at failure is reduced into half of the original, i.e., 0.0005. Fig. 9 shows the results of this model under the superimposed live load as mentioned above. The cracks resulting from the shear strain under this assumption are much

closed to the practical situation. However, the maximum overloading decreases to 142 tonnes, 9% lower than the previous intact model.

The load deflection plot for a point 2.5m from the support for both models (initial and modified weakened model) is shown in Fig. 7. The shear strain for these two models are compared in figs. 8 & 9. The starting deflection of 17.3mm on the load deflection plot represents the deflection due to dead load and prestressing forces. It can be seen that until point 1 on the load-deflection curve, the curves are identical and there is no difference between the initial model and the weakened model. However, as the loading progresses a significant difference develops in the elements that crack. The ultimate superimposed load carrying capacity of 16.16kN/m² and 18.98kN/m² shown in Fig. 7 are points beyond which the solution would not converge anymore.

CONCLUSION

Based on the results of initial model, such severity shear cracks should not have happened on this type of girder bridges, whose design strength lies in high torsional rigidity. The possible reasons for the current cracks may be related to the initial weakened regions near the support (around shear keys) where high shear stress takes place. The cracking propagation diagrams showed in the modified weakened model give the support of this assumption. Another possible reason for shear cracks may be the fatigue due to traffic loading. It is therefore necessary to monitor the crack growth of a few significant cracks and estimate if fatigue may have played a key role. The Finite-Element method and the monitoring system will play a symbiotic role complementing each other. While results from the FE simulation can help in identifying the locations to monitor, data generated from the field will help in calibrating and updating the model from time to time.

It can be concluded that, FE modeling, with suitable material models, can be used to accurately predict the behavior of composite long span girder bridges. The major features of a FE method of analyzing such bridges have been shown. The major nonlinear features of the bridge are successfully captured.

ACKNOWLEDGEMENT

The author would like to thank Amman Municipality, Department of Transportation for making the bridge available for this investigation and providing the required documents. The author also gratefully acknowledge the support received from the Deanship of Engineering, Mutah University for providing the supercomputing resources.

REFERENCES

- [1] ABAQUS theory manual, *Hibbit, Karlsson and Sorensen Inc.*, Pawtucket, R.I. (2002).
- [2] Amman Municipality Report, "Amman Bridges, Maintenance and Repair". *Transportation department, Amman Municipality*, (1994)
- [3] BS5400, Part 5: Concrete and Composite Bridges." Code of Practice for Design of Composite Bridges". *British Standards Institution*, (1979).
- [4] DD ENV 1994-1-1 Eurocode 4, Part 1. "Design of composite steel and concrete structures. General rule and rules for buildings". *British Standards Institution*, London, (1994).
- [5] McDevitt, C. F. & Viest, I. M. "A survey of using steel in combination with other materials", Final report, pp101-117. *Ninth Congress, Int. Ass. for Bridge and Struc. Engineering, Amsterdam*, (1992).
- [6] Podolny, W., "The cause of cracking in post tensioned concrete box girder bridges and retrofit procedures". *PCI Journal*, Vol. 30, No. 2, PP. 82-139, (1985).
- [7] Schilling, C., "Moment-rotation tests of steel bridge girders". *Journal of Structural Engineering, ACSE*, Vol. 114, pp. 134-149, (1988).
- [8] Wang, M., Xu, F., Satpathi, D. and Chen L., "Model testing for multi-span continuous segmental prestressed concrete bridge". *SPIE Conference Smart System for Bridges, Structures and Highways*, Newport Beach, (1999)
- [9] Zhenlei C., Stpathi D. and Ming L., "Numerical investigations of Kishwaukee bridge using ABAQUS". *ABAQUS Users Conference*, pp. 235-246, Chester, UK., (1999).

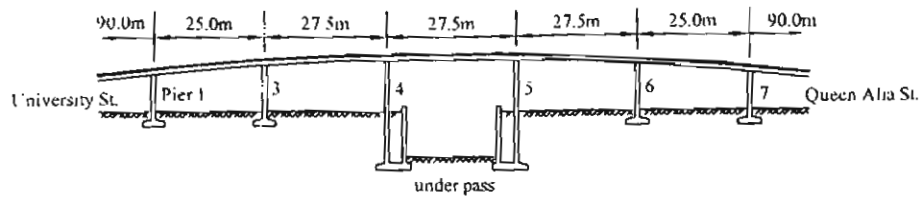


Fig. 1 Schematic layout of sport city overpass bridge

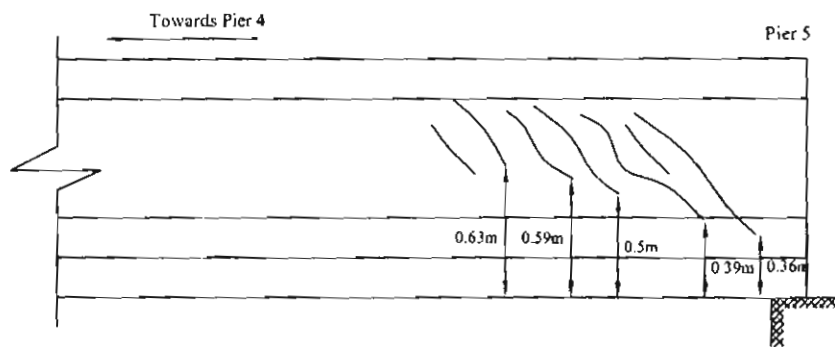


Fig. 2 Crack patterns observed on the east side of the bridge

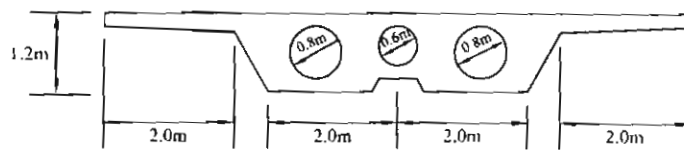


Fig. 3 Dimension of the bridge

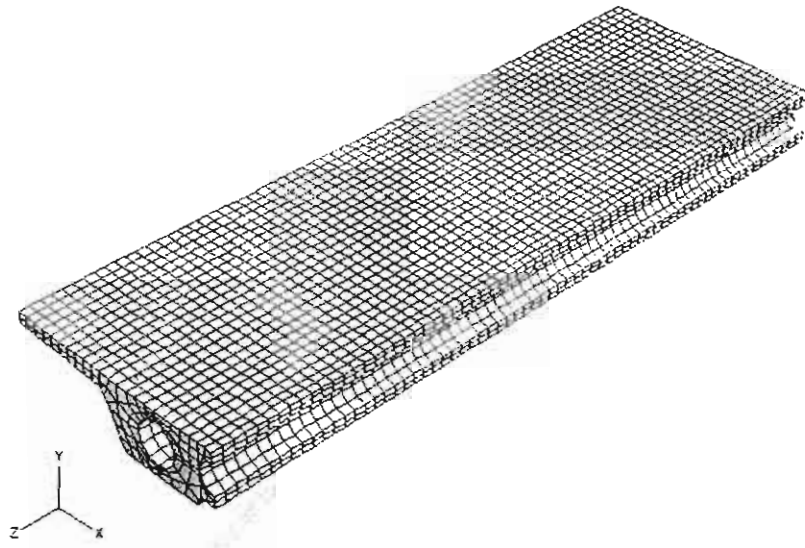


Fig. 4 3D Finite element model

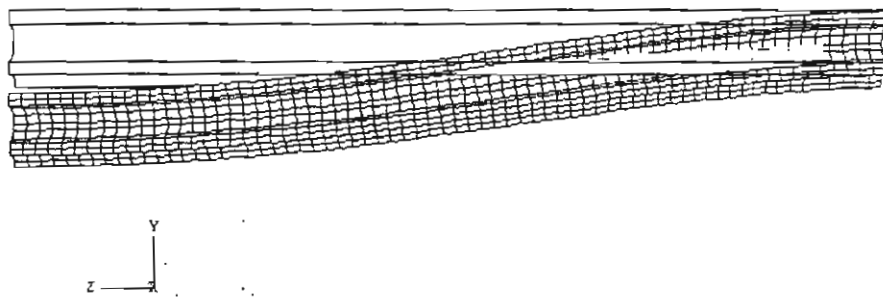


Fig. 5 Deflected shape of the bridge under dead & traffic loads

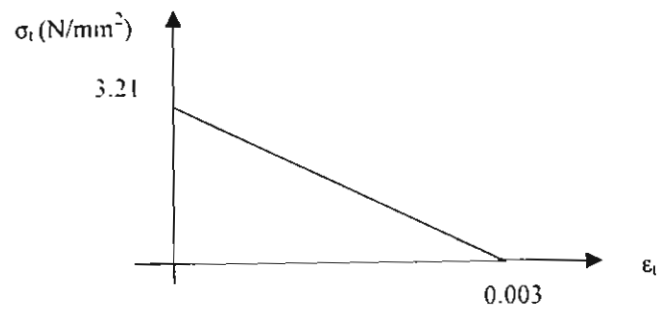


Fig. 6 Post failure stress strain relationship in the FE model

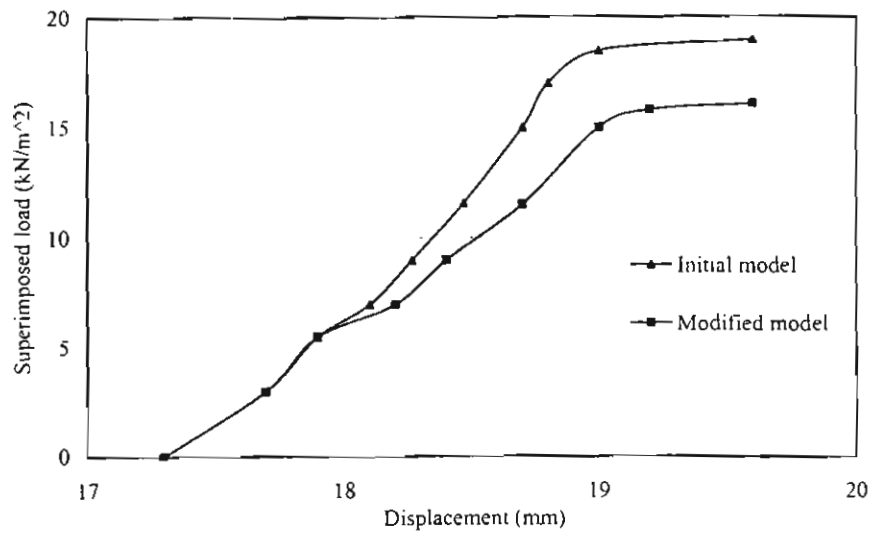


Fig.7 Load-displacement curve for initial model & modified model

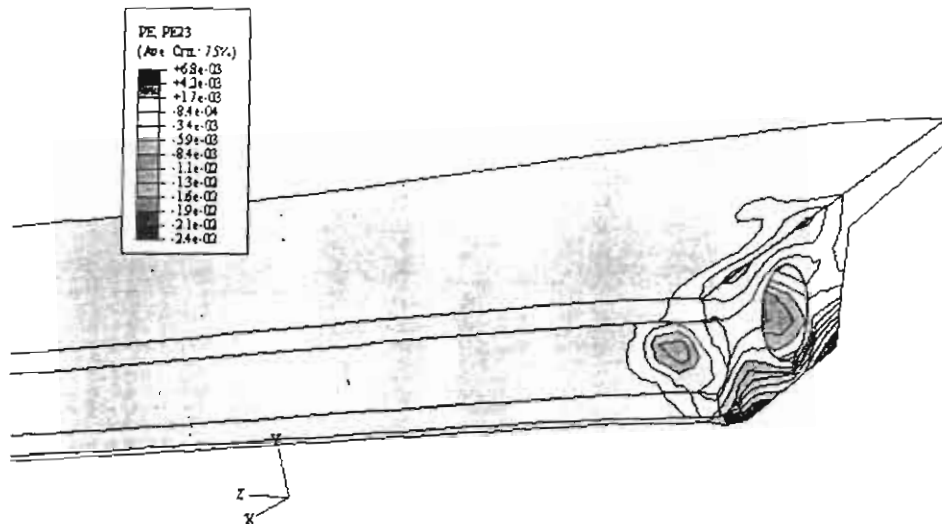


Fig. 8 Plastic shear strain distribution "initial intact model"

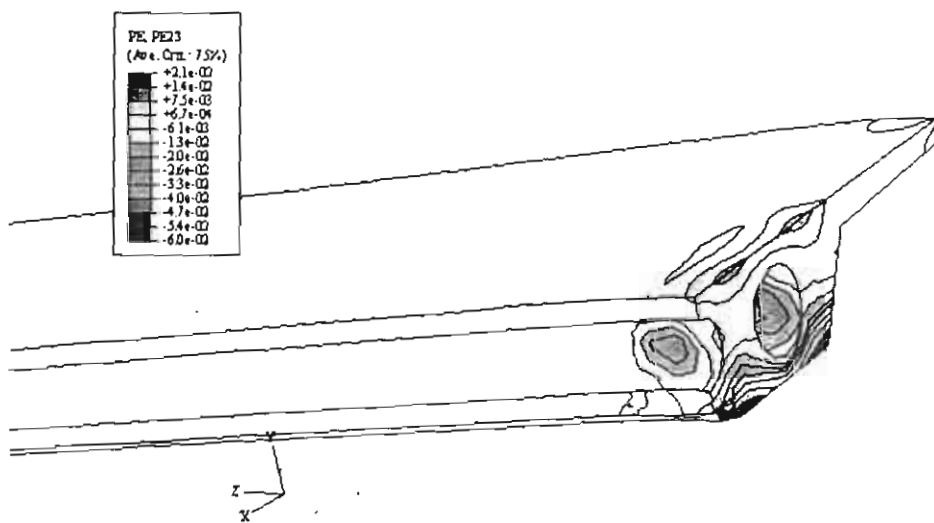


Fig. 9 Plastic shear strain distribution "modified weakened model"

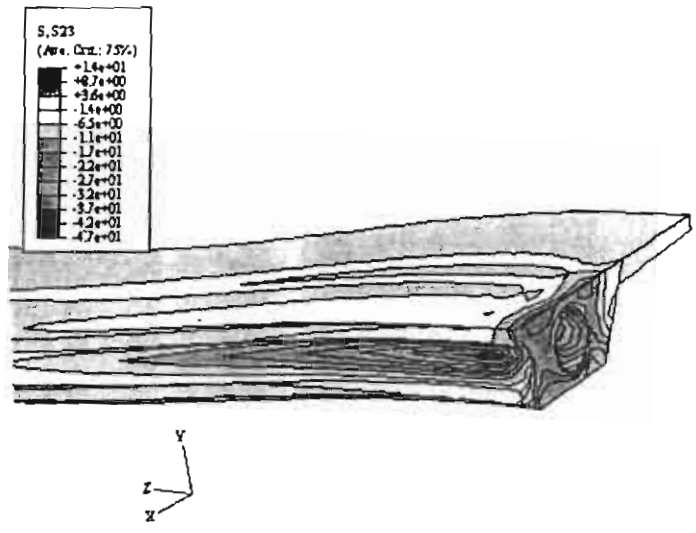


Fig. 10 Shear stress distribution, 3D view

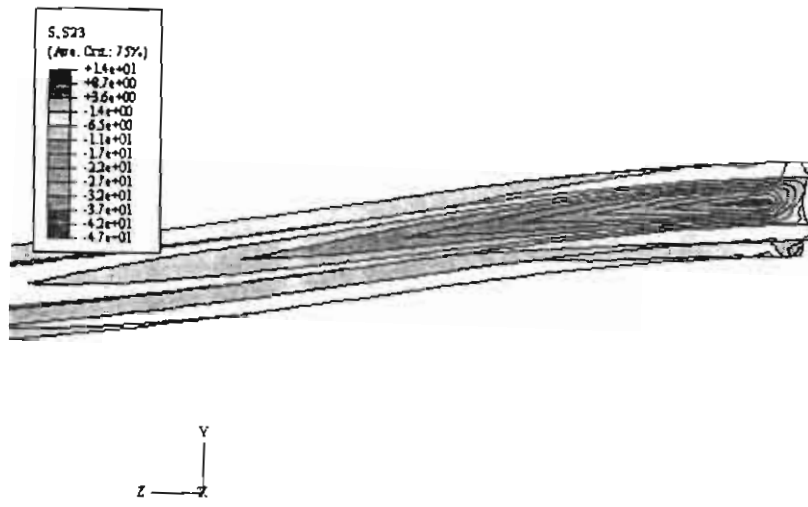


Fig. 11 Shear stress distribution, side view